

Simultaneous Lane-Keeping and Obstacle Avoidance by Combining Model Predictive Control and Control Barrier Functions

Sven Brüggemann*, Drew Steeves*, and Miroslav Krstic

Abstract—In this work, we combine Model Predictive Control (MPC) and Control Barrier Function (CBF) design methods to create a hierarchical control law for simultaneous lane-keeping (LK) and obstacle avoidance (OA): at the low level, MPC performs LK via trajectory tracking during nominal operation; and at the high level, different CBF-based safety filters that ensure both LK and OA are designed and compared across some practical scenarios. In particular, we show that Exponential Safety (ESf) and Prescribed-Time Safety (PTSf) filters, which override the MPC control when necessary, result in feasible Quadratic Programs when safety is prioritized appropriately. We additionally investigate control designs subject to input constraints by using Input-Constrained-CBFs. Finally, we compare the performance of combinations of ESf, PTSf, and their input-constrained counterparts with respect to the LK and OA goals in two simulation studies for early- and late-detected obstacle scenarios.

I. INTRODUCTION

Achieving stability while satisfying state and input constraints makes MPC [1] tremendously appealing to areas such as autonomous systems [2]–[5]. For example, autonomous vehicles tasked with tracking a desired trajectory encounter steering angle input bounds, often employ MPC for motion-planning or trajectory-tracking. However, the constrained optimization problem that forms the backbone of MPC can have prohibitively long computing times. This is problematic for fast-moving safety-critical systems since they demand extremely fast system responses when faced with dangerous system “perturbations”. Additionally, such systems require state constraints that are time-varying and nonconvex, which also risks recursive feasibility.

CBF-based *safety filters* for safety-critical systems have become a popular contender of MPC. Since safety is directly encoded within the CBF, this design method can treat more intricate state constraints while retaining some theoretical guarantees, and prioritizing safety can readily be designed into the safety filter.

In regard to the vehicle *lane-keeping* (LK), MPC is advantageous since, under practical highway-driving assumptions, the (local) vehicle dynamics can be modeled as LTI systems and maximum steering angle inputs are easily handled in the resulting quadratic program (QP). For vehicle *obstacle avoidance* (OA), where (global) nonlinear vehicle dynamics must be considered, CBF-based controllers are desirable since they are computationally cheap, can be designed independent of sampling time, and can natively prioritize safety “violations”.

In this work, we combine these two control design methods to synthesize a two-layer control law which simultaneously performs vehicle LK and OA for highway driving scenarios. We investigate high-performance CBFs which guarantee Prescribed-Time Safety by using time-varying backstepping to impose safety only over the finite time for which the obstacle is ahead of the vehicle. For simultaneous LK and OA while constraining the steering angle to practical values, we also investigate the marriage between MPC, where input constraints are natively considered, and ICCBFs, where they are integrated within the definition of safety. Thanks to our hierarchical structure, manual LK by a human driver can also be handled while providing safety through automatic OA by our CBF-based design only.

Related work

The predominant method to design safety filters has been to use a QP which selects the control input “closest” (in least-squares sense) to a nominal one, subject to linear inequality constraints that enforce safety. The authors of [6], revealed the connection between such Exponential Safety filter (ESf) designs and backstepping through [7]. More recently, the time-varying backstepping methods from [8], [9] were applied in the context of CBF-based safe control design in [10] to generate Prescribed-Time Safety (PTSf), which only invokes safety for as long as it is required. In other words, PTSf maximizes the safe operating envelope of systems to retain high nominal performance (by not requiring the system to be “too safe”); see [10] for a complete description of PTSf.

With the recent Spring of CBFs came their application to safety-critical autonomous systems. For instance, [11] proposes to design CBFs offline through a combination of sum-of-squares program and modeling from [12], and use the related CBF-QP formulation for simultaneous LK and cruise control. In [13], LK is combined with OA by using mixed-integer formulations for Boolean compositions of multiple discrete-time CBFs, but CBF-QP feasibility is not studied.

Combining MPC and CBFs has recently gained traction in the research community. Zhe *et al.* [14] design a CBF-CLF hard constraint for the MPC with proven recursive feasibility, producing stability with safety but without computational/feasibility considerations. Using a multi-rate formulation, in [15] a MPC planner is designed in conjunction with a CBF-QP formulation under the assumption that an ICCBF exists. For OA, the authors in [16] propose a continuous-time CBF as an additional state constraint for a discrete-time nonlinear MPC. The work [17] discusses how discrete-time

*The first and second authors contributed equally to this work.
All authors are with the Mechanical & Aerospace Engineering Department, University of California, San Diego, CA 92093-0411, USA, E-mails: {sbruegge, dsteeves, krstic}@eng.ucsd.edu.

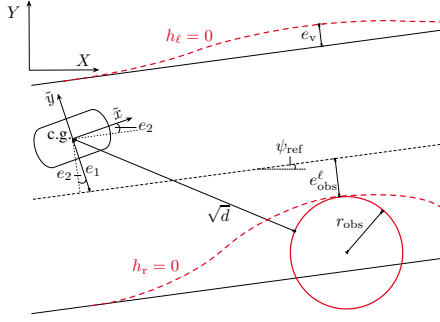


Fig. 1: Obstacle (red circle) on the RHS of the road; lateral distance from center of gravity (c.g.) to the centerline along the vehicle axis, e_1 , and heading error, e_2 ; here both $e_1, e_2 > 0$. The shortest distance from the c.g. to the centerline is $e_1 \cos(e_2)$. The red dashed lines show the boundaries of the safe set, with tuning parameter e_v for possible lane extension. The global coordinates are X, Y ; the local ones are \tilde{x}, \tilde{y} .

CBF constraints jeopardize recursive feasibility. To attempt to tackle this issue, the MPC design in [18] is altered by additionally optimizing over the decay rate of the CBF by using slack variables.

II. LATERAL VEHICLE DYNAMICS

With our underlying goal of LK via trajectory tracking for vehicles during highway-driving conditions, we rely on a dynamic model that governs the local vehicle position, heading and associated velocities (all with respect to the road, see Figure 1). We make the following assumption:

Assumption 1. The longitudinal vehicle vel., v_l , is constant.

With Assumption 1, we obtain the following LTI model that governs the lateral vehicle dynamics [12]:

$$\dot{x}(t) = Ax(t) + Bu(t) + G\dot{\psi}_{\text{ref}}(t), \quad (1)$$

where $x(t) = [e_1 \ \dot{e}_1 \ e_2 \ \dot{e}_2]^\top$, where $u(t)$ is the front wheel steering angle whose magnitude must not exceed some $u_{\text{max}} > 0$, and $\psi_{\text{ref}}(t) \in \mathbb{R}$ is the (desired) reference yaw rate for $t \in \mathbb{R}_{\geq 0}$. We denote the components of A and B by $A = (a_{ij})_{1 \leq i, j \leq 4}$, $B = (b_{i1})_{1 \leq i \leq 4}$, where $b_{i1} = 0$ for $i = \{1, 3\}$, which makes (1) of relative degree two. If the yaw rate $\dot{\psi}_{\text{ref}} \neq 0$, it is impossible to stabilize the longitudinal and angular errors to the origin, since G lies outside $\text{span}(B)$ in general. However, for a fixed yaw rate $\dot{\psi}_{\text{ref}}(t_k)$, as given in [12, Eq. 3.14], the steady state and control are¹

$$u_s(t) = \dot{\psi}_{\text{ref}}(t) \left(\frac{l_f + l_r}{v_l} + k_v v_l \right) \doteq \dot{\psi}_{\text{ref}}(t) \bar{u}_s, \quad (2)$$

$$x_s(t) = \dot{\psi}_{\text{ref}}(t) \begin{bmatrix} 0 & 0 & -\frac{l_r}{v_l} + \alpha_r & 0 \end{bmatrix}^\top \doteq \dot{\psi}_{\text{ref}}(t) \bar{x}_s. \quad (3)$$

Our LK goal is to drive the system to the yaw-rate-dependent steady-state tuple $(x_s(t), u_s(t))$, which we detail next using an MPC-based control design.

¹ l_r (l_f) is the distance from the center of gravity to the rear (front) tires (resp.), k_v the under-steer gradient, and $\alpha_r \psi_{\text{ref}}(t)$ is the slip angle of the rear tires.

III. HIGH-LEVEL SAFETY FILTER

In this section, we assume that a nominal control input performs LK while driving around a known track (cf. Section IV for our MPC-based LK design).

Our high-level safety filter is designed to perform both of the LK and OA tasks by employing barrier functions which encode these objectives. It is implemented by the common QP-based approach

$$\begin{aligned} u_{\text{safe}} &= \arg \min_{w \in \mathbb{R}} |w - u_{\text{nominal}}|^2 \\ \text{s.t.} \quad &a_i + b_i w \geq 0, \\ &a_k + b_k w \geq 0, \end{aligned} \quad (4)$$

where one inequality constraint is used to encode the LK objective, and the other encodes the OA objective. In order to generate safety overriding controllers which can simultaneously satisfy both objectives (and in particular, satisfy the so-called control-sharing property [19], which is a necessary and sufficient condition for (4) to be feasible), we propose a barrier function which smoothly transitions from one of the roadway lane barriers to one encapsulating the obstacle, whereas the other lane barrier either remains the same or expands in a direction away from the obstacle (see Figure 1).

Note that lane modification is not inherent or immediately available to the MPC design method: in most applications, modifying any existing state constraints in real-time brings into question recursive feasibility. It is the combination of a low-level MPC design and a high-level safety filter design that allows us to prescribe how the vehicle passes the obstacle while retaining theoretical guarantees, and allows us to characterize what violation may be needed with respect to the original lane barriers in order to ensure that (4) remains feasible.

A. Control Barrier Function Design for LK and OA

We begin by designing our barrier functions (BFs) that encode vehicle safety w.r.t. LK and OA. We first define the squared relative distance from vehicle to obstacle,

$$d(e_1, e_2) := (X_{\text{car}}(e_1, e_2) - X_{\text{obs}})^2 + (Y_{\text{car}}(e_1, e_2) - Y_{\text{obs}})^2 - r_{\text{obs}}^2,$$

where r_{obs} denotes the radius of the obstacle-encompassing circle, and $(X_{\text{car}}, Y_{\text{car}})$, $(X_{\text{obs}}, Y_{\text{obs}})$ denote the global coordinates of the vehicle and the obstacle, respectively. Next, we define the smooth step function which depends on the relative distance, $d(e_1, e_2)$, and the parameter $\delta_2 > 0$ which is the relative detection distance:

$$\Phi(d) = \begin{cases} 0, & d \geq \delta_2^2, \\ \exp\left(1 - \frac{\delta_2^2}{d}\right), & 0 < d < \delta_2^2, \\ 1, & d \leq 0. \end{cases} \quad (5)$$

For $w_l > 0$ denoting the width of the lane and e_{obs}^ℓ denoting the shortest distance of the obstacle-encompassing circle to the centerline (see Figure 1), we define the left BF (ensuring LK or a certain violation of of LK)

$$h_\ell := \Phi(d) \left(\frac{w_l}{2} - e_1 \cos(e_2) + e_v \right) + (1 - \Phi(d)) \left(\frac{w_l}{2} - e_1 \cos(e_2) \right), \quad (6)$$

where $e_v \geq 0$ is a design parameter which allows the vehicle to utilize a portion of the highway shoulder or a left-hand lane (assuming no oncoming traffic). By selecting $e_v = 0$, the left barrier simplifies to $h_\ell(e_1, e_2) = \frac{w_1}{2} - e_1$, that is, it remains constant regardless of the vehicle's proximity to the obstacle. We define the right BF (ensuring OA) as

$$h_r := \Phi(d) (e_1 \cos(e_2) - e_{\text{obs}}^\ell) + (1 - \Phi(d)) \left(\frac{w_1}{2} + e_1 \cos(e_2) \right). \quad (7)$$

While the choice $e_v = 0$ is made throughout Section V with success, to establish theoretical safety guarantees (cf. Lemma 1 and Remark 1), we must prioritize OA over LK by selecting $e_v > 0$.

For the purpose of presentation clarity, we assume w.l.o.g. that the (geometric) center of the obstacle-encompassing circle is on the right side of the road centerline, i.e., that $e_{\text{obs}}^\ell < 0$, and that we seek to pass on the left side of the obstacle. Figure 1 depicts the left and right BFs as red dashed lines. We define the safe sets

$$\mathcal{S}_\ell := \{x \in \mathbb{R}^4 \mid h_\ell(e_1, e_2) \geq 0\}, \quad \mathcal{S}_r := \{x \in \mathbb{R}^4 \mid h_r(e_1, e_2) \geq 0\};$$

our goal is to design MPC-overriding control laws which renders $\mathcal{S}_\ell \cap \mathcal{S}_r$ positively-invariant.

While the MPC design for lane-keeping is performed using the linear local dynamics (1), the safety filter design, which invokes the vehicle's global position in (5), involves the vehicle's nonlinear dynamics: the vehicle coordinates $(X_{\text{car}}, Y_{\text{car}})$ are related to the rel.-deg.-two system (1) by

$$\begin{aligned} \frac{dX_{\text{car}}}{dt}(e_1, \dot{e}_1, e_2) &= v_1 \cos(e_2 + \psi_r) - (\dot{e}_1 - v_1 e_2) \sin(e_2 + \psi_r), \\ \frac{dY_{\text{car}}}{dt}(e_1, \dot{e}_1, e_2) &= v_1 \sin(e_2 + \psi_r) + (\dot{e}_1 - v_1 e_2) \cos(e_2 + \psi_r). \end{aligned}$$

Hence, it follows from the vehicle's (global) velocities and the dynamics that (6), (7) are rel.-deg.-two CBFs.

B. Exponential Safety by (Time-Invariant) Backstepping

Next, we introduce the time-invariant backstepping method which leads to explicit characterizations for the safety overriding controllers, referred to as ESf control designs, which render either \mathcal{S}_ℓ or \mathcal{S}_r positively-invariant. This method is a specific case of more general CBF-safety designs, where the inequalities in (4) are typically constructed using class- \mathcal{K} functions of the CBFs and their derivatives; the backstepping framework presents a direct connection between safety conservatism and performance via gain tuning (cf. Section III-C for details).

For $i \in \{\ell, r\}$, we define

$$h_{i,1}(e_1, e_2) = h_i(e_1, e_2), \quad (8)$$

$$h_{i,2}(x) = \frac{d}{dt} h_{i,1}(x) + c_{i,1} h_{i,1}(e_1, e_2); \quad (9)$$

by selecting the gains to satisfy

$$c_{i,1} > \max \left\{ 0, -\frac{\frac{d}{dt} h_{i,1}(x(0))}{h_{i,1}(e_1(0), e_2(0))} \right\}, \quad (10)$$

we ensure that $h_{i,2}(x(0)) > 0$. To guarantee $h_{i,1}(e_1(t), e_2(t)) \geq 0$ for all $t \in [0, \infty)$, or in other words, that \mathcal{S}_i remains positively-invariant indefinitely, we must additionally show that

$$\frac{d}{dt} h_{i,2} + c_{i,2} h_{i,2} \geq 0, \quad (11)$$

for $c_{i,2} > 0$; indeed, the barrier constraint (11) is exactly [19, Equ. 7] for $r = 2$, $a_1 = c_{i,1} + c_{i,2}$, and $a_2 = c_{i,1} c_{i,2}$, since

$$c_{i,2} h_{i,2} = c_{i,2} \left(\frac{d}{dt} h_{i,1} + c_{i,1} h_{i,1} \right) =: c_{i,2} L_f h_{i,1} + c_{i,1} c_{i,2} h_{i,1}, \quad (12)$$

$$\frac{d}{dt} h_{i,2} =: L_f^2 h_{i,1} + L_g L_f h_{i,1} u + c_{i,1} L_f h_{i,1}. \quad (13)$$

A safety filter can then be designed as the QP (4), with $a_i := L_f^2 h_{i,1} + (c_{i,1} + c_{i,2}) L_f h_{i,1} + c_{i,1} c_{i,2} h_{i,1}$, $b_i := L_g L_f h_{i,1}$, $a_k = 0$, and $b_k = 0$. Equivalently, we can select

$$u_{i,\text{override}} = -\frac{L_f^2 h_{i,1} + (c_{i,1} + c_{i,2}) L_f h_{i,1} + c_{i,1} c_{i,2} h_{i,1}}{L_g L_f h_{i,1}}, \quad (14)$$

which is well-defined so long as $L_g L_f h_{i,1}$ never equals zero, and implement

$$\begin{aligned} u_{\text{safe}} &= \arg \min_{w \in \mathbb{R}} |w - u_{\text{MPC}}|^2 \\ \text{s.t. } w &\geq u_{\text{override}}. \end{aligned} \quad (15)$$

In scenarios where $L_g L_f h_{i,1} = 0$, the *validity* of h_i as a CBF depends on whether (11) holds despite $L_g L_f h_{i,1} = 0$ (that is, h_i is a *valid* CBF if (11) holds true when $h_i \geq 0$ and despite the control having no effect on (11)).

In practice, verifying the validity of a candidate CBF is difficult when $L_g L_f h_{i,1} = 0$ at some time instances, since the system states are arbitrary and the sign of the Lie derivative terms in (12), (13) may be state-dependent and large (as is the case here for the sinusoidal nonlinearities). This is often resolved in practice (e.g., [20]–[22]) by modifying the barrier constraint in (4) to be a soft constraint. For the CBFs (6) and (7), we compute

$$\begin{aligned} L_g L_f h_{\ell,1} &= -b_{21} \cos(e_2) + b_{41} e_1 \sin(e_2) + \frac{2b_{21}\delta_2^2}{(\delta_2^2 - d(e_1))^2} \Phi(d(e_1)) e_v \\ &\times \left[(X_{\text{car}} - X_{\text{obs}}) \sin(e_2 + \psi_r) - (Y_{\text{car}} - Y_{\text{obs}}) \cos(e_2 + \psi_r) \right], \end{aligned} \quad (16)$$

and

$$L_g L_f h_{r,1} = b_{21} \cos(e_2) - b_{41} e_1 \sin(e_2) - \frac{2b_{21}\delta_2^2}{(\delta_2^2 - d(e_1))^2} \Phi(d(e_1)) \quad (17)$$

$$\times \left(\frac{w_1}{2} + e_{\text{obs}}^\ell \right) [(X_{\text{car}} - X_{\text{obs}}) \sin(e_2 + \psi_r) - (Y_{\text{car}} - Y_{\text{obs}}) \cos(e_2 + \psi_r)],$$

which *may* equate to zero for certain vehicle headings, heading errors, and relative distances between vehicle and obstacle; this is one caveat of using Assumption 1 to obtain (1) (which effectively renders our nonholonomic model as *underactuated*) since otherwise, another control term would appear to prevent $L_g L_f h_{i,1} = 0$. However, in the numerous closed-loop simulation studies performed (some of which are featured in Section V), $L_g L_f h_{i,1} = 0$ never

occured. Note that $\lim_{d(e_1) \rightarrow \delta_2^2} \frac{\Phi(d(e_1))}{(\delta_2^2 - d(e_1))^k} = 0$ for any $k \in \mathbb{N}$.

By selecting $e_v = (\frac{w_l}{2} + e_{\text{obs}}^\ell)$ in (16), we obtain $L_g L_f h_{\ell,1} = -L_g L_f h_{r,1}$, which generates the following result.

Lemma 1. *Suppose a vehicle governed by (1) detects an obstacle and has access to $d(e_1, e_2)$. Under Assumption 1, and if $L_g L_f h_{i,1}(x) \neq 0$ for all $x \in \mathcal{S}_i$, $i \in \{\ell, r\}$, if we permit the left-lane expansion*

$$e_v = \left(\frac{w_l}{2} + e_{\text{obs}}^\ell\right) > 0, \quad \text{where } e_{\text{obs}}^\ell < 0, \quad (18)$$

then for $i \in \{\ell, r\}$ and the overriding controller (14), if we select $c_{\ell,j} = c_{r,j} > 0$ for $j = 1, 2$, then

$$u_{\ell, \text{override}} - u_{r, \text{override}} = (L_g L_f h_{\ell,1})^{-1} c_{\ell,1} c_{\ell,2} w_l. \quad (19)$$

In other words, the CBFs (6), (7) have the control-sharing property [19], and hence generate the feasible QP

$$u_{\text{safe}} = \arg \min_{w \in \mathbb{R}} |w - u_{\text{MPC}}|^2 \quad (20)$$

$$\text{s.t. } u_{r, \text{override}} \leq w \leq u_{\ell, \text{override}},$$

when $L_g L_f h_{\ell,1} < 0$ (otherwise, the barrier inequalities must be flipped). Moreover, if we additionally select $c_{\ell,1}$ to satisfy (10), then the safety filter (20) ensures that $\mathcal{S}_\ell \cap \mathcal{S}_r \neq \emptyset$ remains positively-invariant for (1) for all times provided that $x(0) \in \mathcal{S}_\ell \cap \mathcal{S}_r$, and (1) with (20) is ESf.

The proof of Lemma 1 directly follows from computing the overriding controllers, the selection (18), and both [19, Thm. 1], [6, Cor. 2].

Remark 1. While Lemma 1 prioritizes OA over LK by permitting the vehicle to “violate” the left lane marker by up to an additional half lane width in (18), these conditions are encountered in practice: vehicles can often access a left-hand lane (assuming no oncoming vehicles) or a highway shoulder. The result illustrates the conservativeness required to establish theoretical guarantees when using multiple CBFs, since (19) $e_v = 0$ was sufficient in our simulation studies.

C. Balancing Performance and Safety by ESf and PTSf

We classify “high performance” as imposing the minimum amount of control intervention to retain safety. If we select large gains $c_{i,j}$ for $i \in \{\ell, r\}$, $j = 1, 2$, then the exponential decay in time of $h_{i,j}$ will be large, causing the safe operating envelope \mathcal{S}_i to become larger. In other words, a larger gain makes safety less conservative, causing less intervention by the safety filter with the nominal controller, and allowing the vehicle to perform as intended. One caveat to selecting large constant gains is that the initial behavior of the safety filter (20) can exhibit a drastic intervention when the nominal control is first unsafe, as is exhibited in Figure 3 and discussed therein; this behavior is not an issue with smaller gains. These large interventions are particularly problematic when actuator constraints are present. To circumvent them while retaining the intended closed-loop performance, we investigate PTSf by using time-varying-gains for (1), (20)

which start small (when $h_{i,j}$ is large) and grow large (as $h_{i,j}$ becomes small, as the vehicle approaches the obstacle).

D. Prescribed-Time Safety by Time-Varying Backstepping

Since the obstacle threatens the safe operation of the vehicle only while the vehicle is moving towards it, the OA problem is finite-time in nature, and we would like the safety filter to only perform LK after passing the obstacle. One way to accomplish this is to revert from the OA barrier constraint back to one which encodes LK safety; this behavior is in fact exhibited in a smooth fashion by our CBF design (7). But we would also like to balance safety and performance via gain tuning without producing large overriding control inputs. To this end, we turn to PTSf designs.

PTSf uses time-varying gains to not only balance performance and safety by small overriding inputs, but to enforce safety only for as long as required. PTSf designs retain $h_{i,j}(t) \geq 0$ but drive $h_{i,j}(t) \rightarrow 0$ within a finite time that can be a priori prescribed, for $i \in \{\ell, r\}$ and $j = 1, 2$; in contrast, ESf requires $t \rightarrow \infty$ for $h_{i,j}(t) \rightarrow 0$ (see [23] for a more extensive discussion on PTSf).

PTSf designs rely on the following time-varying blow-up function

$$\mu_2(t - t_{\text{obs}}, T) := \frac{1}{\left(1 - \frac{t - t_{\text{obs}}}{T}\right)^2}, \quad t \in [t_{\text{obs}}, t_{\text{obs}} + T], \quad (21)$$

which equals one at the detection time t_{obs} (when $d(e_1, e_2) = \delta_2^2$ in (5)) but equals infinity at the passing time $t_{\text{obs}} + T$.

Since the longitudinal vehicle velocity v_1 is constant, we can estimate the passing time quite accurately for highway driving scenarios, by using the following relation to numerically solve for the T :

$$d_{\text{obs}}^{\text{path}} = \left[\left(\int_{t_{\text{obs}}}^T v_1 \cos(\psi_{\text{ref}}(t)) dt \right)^2 + \left(\int_{t_{\text{obs}}}^T v_1 \sin(\psi_{\text{ref}}(t)) dt \right)^2 \right]^{1/2}, \quad (22)$$

where $d_{\text{obs}}^{\text{path}}$ is the relative distance between the end of the obstacle and the vehicle along the path at time $t = t_{\text{obs}}$.

We now exchange the constant gains in (14) with the following time-varying gains: for $t \in [t_{\text{obs}}, t_{\text{obs}} + T)$, we define

$$c_{i,j}(t) = c_{i,j}^0 \mu_2(t - t_{\text{obs}}, T), \quad i \in \{\ell, r\}, j = 1, 2, \quad (23)$$

where $c_{i,j}^0 > 0$ also satisfying (10) are the *initial* gains at detection time and can be chosen to be as small as possible while retaining a large safe operating envelope. Employing these time-varying gains generates the following result, which is a consequence of Lemma 1 and the treatment in the proof of [23, Thm. 1].

Proposition 1. *Suppose a vehicle governed by (1) detects an obstacle and has access to $d(e_1, e_2)$. Under Assumption 1, and if $L_g L_f h_{i,1}(x) \neq 0$ for all $x \in \mathcal{S}_i$, $i \in \{\ell, r\}$, if we select (18), then for $i \in \{\ell, r\}$ and*

$$u_{i, \text{override}} = - \frac{L_f^2 h_{i,1} + (c_{i,1} + c_{i,2}) L_f h_{i,1} + (\dot{c}_{i,1} + c_{i,1} c_{i,2}) h_{i,1}}{L_g L_f h_{i,1}}, \quad (24)$$

if we select $c_{\ell,j} = c_{r,j} > 0$ for $j = 1, 2$, then

$$u_{\ell,\text{override}} - u_{r,\text{override}} = (L_g L_f h_{\ell,1})^{-1} (\dot{c}_{\ell,1} + c_{\ell,1} c_{\ell,2}) w_{\ell}. \quad (25)$$

In other words, the CBFs (6), (7) have the control-sharing property, and hence generate the feasible QP

$$\begin{aligned} u_{\text{safe}} &= \arg \min_{w \in \mathbb{R}} |w - u_{\text{MPC}}|^2 \\ \text{s.t. } u_{r,\text{override}} &\leq w \leq u_{\ell,\text{override}}, \end{aligned} \quad (26)$$

when $L_g L_f h_{\ell,1} < 0$ (otherwise, the barrier inequalities must be flipped). If we additionally select $c_{\ell,1}$ to satisfy (10), then the safety filter (26) ensures that $\mathcal{S}_{\ell} \cap \mathcal{S}_r \neq \emptyset$ remains positively-invariant for (1) over the interval $[t_{\text{obs}}, t_{\text{obs}} + T]$ provided that $x(t_{\text{obs}}) \in \mathcal{S}_{\ell} \cap \mathcal{S}_r$, and (1) with (26) is PTSf. Moreover, the time-varying overriding control laws are uniformly bounded for $t \in [t_{\text{obs}}, t_{\text{obs}} + T]$.

Absent from Proposition 1 are closed-loop system guarantees after the passing time $t_{\text{obs}} + T$, which are required since our LK objective has not expired. Handling the PTSf filter behavior after the passing time can be done using a smooth ramp function, as detailed in [23, Eqs. (10), (11)], and as implemented in Section V.

Moreover, the time-varying filter (20) is not required for the LK objective, since LK persists after the passing time. In Section V, we use (14) for $i = \ell$ and we use (24) for $i = r$; however, with this combination, the control-sharing property becomes difficult to establish and requires further study which, due to space constraints, will be featured elsewhere.

E. Input-Constrained CBFs (ICCBFs)

Given our hierarchical approach to solve the LK and OA problems for vehicles travelling on the highway, one glaring incompatibility between MPC- and CBF-based control designs is that the former can handle input constraints, whereas up until recently, the latter could not.

The work [24] introduces ICCBF, whose designs that are similar to CBF designs, except they restrict the safe sets \mathcal{S}_i further by iteratively removing states from which system safety can only be achieved by violating the input constraints. In the (time-invariant) backstepping framework, the first iteration of the ICCBF design replaces (9), (11) by

$$\frac{d}{dt} h_{i,1}(x) = -c_{i,1} h_{i,1}(e_1, e_2) + h_{i,2}(x), \quad (27)$$

$$\frac{d}{dt} h_{i,2} \geq -c_{i,2} h_{i,2} - \inf_{|u| \leq u_{\text{max}}} \{L_g L_f h_{i,1} u\}, \quad (28)$$

which translates to the BF constraint

$$\begin{aligned} b_{i,2}(x) &:= L_f^2 h_{i,1} + (c_{i,1} + c_{i,2}) L_f h_{i,1} \\ &\quad + c_{i,1} c_{i,2} h_{i,1} + \inf_{|u| \leq u_{\text{max}}} \{L_g L_f h_{i,1} u\} \geq 0; \end{aligned} \quad (29)$$

the manipulation (29) effectively treats the control term as a disturbance and adds a margin of safety to the dynamics governing $h_{i,2}$ equal to the disturbance's upper bound. Notice that the relative degree of the ICCBF is no longer two, as is the case for the CBFs in Sections III-B and III-D; indeed,

the ICCBF methodology iterates backstepping *at least once more* by enforcing (similar to (11)) $\frac{d}{dt} b_{i,2} + c_{i,3} b_{i,2} \geq 0$ for $c_{i,3} > 0$, which is equivalent to the CBF constraint

$$L_f b_{i,2}(x) + L_g b_{i,2}(x) u + c_{i,3} b_{i,2}(x) \geq 0. \quad (30)$$

We say that $b_{i,2}$ is an ICCBF if

$$L_f b_{i,2}(x) + \sup_{|u| \leq u_{\text{max}}} \{L_g b_{i,2}(x) u\} + c_{i,3} b_{i,2}(x) \geq 0 \quad (31)$$

holds *only* on the set $x \in \mathcal{S}_i \cap \{b_{i,2}(x) \geq 0\}$ (see [24, Def. 4] for details).

As for standard CBFs, validating (31) is difficult in practice. However, minimizing the left-hand side of (31) is a test to invalidate candidate ICCBFs; in these cases, the authors of [24] propose to iterate the backstepping procedure $M \in \mathbb{N}$ times to further restrict the safe set (yet existence of an M guaranteeing (31) is an open problem).

For our LK and OA problems for highway-driving vehicles, we combine the methodologies behind ICCBFs and PTSf (which we call PT-ICCBFs) to investigate performance and safety through simulation studies. While we do not provide a theoretical study of this combination of safety filter designs due to a lack of space, we remark that the interpretation of the control term in (28) as a worst-case disturbance casts the problem into one which was studied in [9] using time-varying backstepping, where positive results were reported.

IV. LOW-LEVEL MPC

The low-level MPC ensures LK via trajectory tracking and runs at a lower sampling rate than the safety-critical control. Hence, we discretize the system (1) and design the control law

$$u(t_k) = u_s(t_k) + v(t_k), \quad (32)$$

where $u_s(t_k)$ is sampled from (2). The evolution of the discrete-time error signal $e_x(t_k) = x(t_k) - x_s(t_k)$ is then described by

$$e_x(t_{k+1}) = A_d e_x(t_k) + B_d v(t_k) - w(t_k),$$

where subscript d denotes the matrices related to the discretized dynamics of (1), using a zero-order-hold, and w denotes the system's deviation from the steady state (3) due to a change in desired yaw rate over one time step. It is defined as

$$w(t_k) = A_d \Delta x_s(t_k) + B_d \Delta u_s(t_k) + G_d \Delta \dot{\psi}_{\text{ref}}(t_k), \quad (33)$$

with $\Delta x_s(t_k) = x_s(t_{k+1}) - x_s(t_k)$, $\Delta u_s(t_k) = u_s(t_{k+1}) - u_s(t_k)$, $\Delta \dot{\psi}_{\text{ref}}(t_k) = \dot{\psi}_{\text{ref}}(t_{k+1}) - \dot{\psi}_{\text{ref}}(t_k)$. Let the MPC-related cost function be

$$\begin{aligned} J_N(e_x(t_k), \mathbf{v}(t_k), \dot{\psi}_{\text{ref}}(t_k)) &= |e_x(t_{N|k})|_P^2 \\ &\quad + \sum_{i=0}^{N-1} |e_x(t_{i|k})|_Q^2 + |v(t_{i|k})|_R^2, \end{aligned}$$

$$\text{s.t. } e_x(t_{0|k}) = e(t_k),$$

$$e_x(t_{i+1|k}) = A_d e_x(t_{i|k}) + B_d v(t_{i|k}) - w(t_k),$$

where $\mathbf{v}(t_k) \doteq \{v(t_{0|k}), \dots, v(t_{N-1|k})\}$ and $\dot{\psi}_{\text{ref}}(t_k) \doteq \{\dot{\psi}_{\text{ref}}(t_k), \dots, \dot{\psi}_{\text{ref}}(t_{N-1|k})\}$. The matrices Q and R are positive definite, $|x|_Q \doteq \sqrt{x^\top Q x}$, and for $i \in \{0, \dots, N-1\}$ we define the set of admissible control inputs by

$$\mathcal{V}_{t_k} \doteq \{\mathbf{v}(t_k) : |u_s(t_{k+i}) + v(t_{i|k})| \leq u_{\max}\}.$$

At every time instance, the MPC solves the optimization problem $\mathcal{P}(t_k)$:

$$\min_{\mathbf{v}(t_k) \in \mathcal{V}_{t_k}} J_N(e_x(t_k), \mathbf{v}(t_k), \dot{\psi}_{\text{ref}}(t_k)) \text{ s.t. } e(t_{N|k}) \in \mathcal{E},$$

with $\mathcal{E} \in \mathbb{R}^{n_x}$ as the terminal constraint set on the state characterized later.

Remark 2. Since e_1 is the lateral error along the local vehicle axis (see Figure 1), state constraints would result in a non-convex nonlinear program; hence, we delegate this responsibility to the safety filter.

For obtaining recursive feasibility and convergence, we make the following standard assumptions.

Assumption 2. (A_d, B_d) is controllable.

Assumption 3 (Bounded admissible reference). There exist positive $c_\psi < u_{\max}/\bar{u}_s$ and $c_{\Delta\psi}$ such that for all t_k ,

$$|\dot{\psi}_{\text{ref}}(t_k)| \leq c_\psi, \quad |\Delta\dot{\psi}_{\text{ref}}(t_k)| \leq c_{\Delta\psi}.$$

Assumption 3 ensures that the steady-state tuple $(x_s(\dot{\psi}_{\text{ref}}), u_s(\dot{\psi}_{\text{ref}}))$ is bounded and varies sufficiently slow. In particular, the upper bound on c_ψ implies that the reference yaw rate is such that the corresponding steady-state input, $u_s(t_k) = \dot{\psi}_{\text{ref}}(t_k)\bar{u}_s$, is in the interior of the constraint set.

Lemma 2. Assumption 3 implies that in (33) $w(t_k) \in \mathcal{W}$ for all t_k , where the polytope

$$\mathcal{W} = \left\{ w \in \mathbb{R}^{n_x} : \begin{bmatrix} I \\ -I \end{bmatrix} w \leq c_{\Delta\psi} \begin{bmatrix} I \\ I \end{bmatrix} b \right\},$$

with $b = A_d \bar{x}_s + B_d \bar{u}_s + G_d$. Furthermore, the polytopic set of admissible control inputs $v(t_k)$ from (32),

$$\bar{\mathcal{V}} \doteq \left\{ v \in \mathbb{R} : \begin{bmatrix} 1 \\ -1 \end{bmatrix} v \leq \begin{bmatrix} u_{\max} - c_\psi \bar{u}_s \\ u_{\max} + c_\psi \bar{u}_s \end{bmatrix} \right\},$$

is non-empty.

Note that $\bar{\mathcal{V}}$ describes the set of controls $v(t_k)$ that are admissible at all times, i.e., $\bar{\mathcal{V}} \subset \mathcal{V}_{t_k}$ for all t_k . On the other hand, \mathcal{W} characterizes the maximum plant deflection related to a change in desired yaw rate. In this fashion, they represent the worst case scenario for the tracking controller and hence the basis for the so-called *maximal invariant constraint admissible (MICA)* set:

$$\mathcal{E} = \{e \in \mathbb{R}^{n_x} : (A_d - B_d K) - w \in \mathcal{E}, K e \in \bar{\mathcal{V}}, w \in \mathcal{W}\},$$

where K is chosen such that $(A_d - B_d K)$ is Hurwitz. The MICA set can be computed using, e.g., [25], [26].

Assumption 4. The bound $c_{\Delta\psi}$ in Assumption 3 renders $\mathcal{E} \neq \emptyset$.

This assumption requires the yaw rate to vary sufficiently slow. Note that Assumptions 3 and 4 ensure that there exists a $c_{\Delta\psi} > 0$ such that $\mathcal{E} \neq \emptyset$ is indeed satisfied.

Proposition 2 (Recursive feasibility). Suppose Assumptions 2–4 hold. If problem $\mathcal{P}(t_0)$ is feasible, then $\mathcal{P}(t_k)$ is feasible for all t_k .

The proof is standard for \mathcal{E} being MICA, see e.g. [1], [25], [27]. Recursive feasibility ensures that the MPC generates a control input at all time instances t_k despite a time-varying road curvature and hence desired yaw rate.

Remark 3 (Stability). The notion of stability usually assumes a fixed steady state. For any fixed $\dot{\psi}_{\text{ref}}$ satisfying Assumption 3 the MPC renders $x_s(\dot{\psi}_{\text{ref}})$ exponentially stable if, e.g., P of the terminal cost satisfies the related Riccati equation. We refer to [28] for the proof and an overview of methods achieving stability, e.g., scaling the terminal cost and dropping the terminal constraint [29] for computational improvement.

V. SIMULATIONS

In our simulation studies, we use typical highway conditions in the U.S.² [30], and assume a constant longitudinal vehicle velocity of $v_l = 20\text{m/s}$ while being controlled by the MPC- and CBF-based safety filter in (20) or (26) on a single-lane road (with $e_v = 0$ in (6)). The desired path (the center line) is reachable given the vehicle dynamics and steering constraints. The related reference yaw rate and acceleration are provided as time-dependent discrete points and interpolated for the continuous-time safety filter. For feasibility of the MPC³, instead of using slack variables as in Remark 3, we choose a terminal cost sufficiently large to ensure that the terminal set \mathcal{E} is reached. Due to the high velocity, in some simulations, we impose $u_{\max} = 5^\circ$ and saturate the controls accordingly. The dynamics from (1) are used as a plant model for the MPC, which is applied at a frequency of 20Hz; the safety filter is computed continuously. The passing time $t_{\text{obs}} + T$ is approximated using (22), or more precisely, using the longitudinal velocity and the relative distance along the desired path to the orthogonal projection of the obstacle onto the path. The car width is encoded within the lane width, w_l , and obstacle radius r_{obs} . We present two simulation studies: A. comparing ESf and PTSf (while using ESf for LK) during early obstacle detection scenarios, and; B. comparing input-constrained PTSf and PT-ICCBF (while using ICCBF for LK) during late obstacle detection scenarios.

A. ESf and PTSf during early obstacle detection

We assume the obstacle is detected 40m ahead and use the ESf design in Section III-B for LK. We compare the closed-loop performance of MPC with ESf OA to that of MPC with PTSf OA. In Figure 2, we observe that both designs successfully avoid the obstacle while staying on

²minimum road radius of 1800m, lane width of 3.7m

³Horizon $N = 30$; MPC implemented as QP

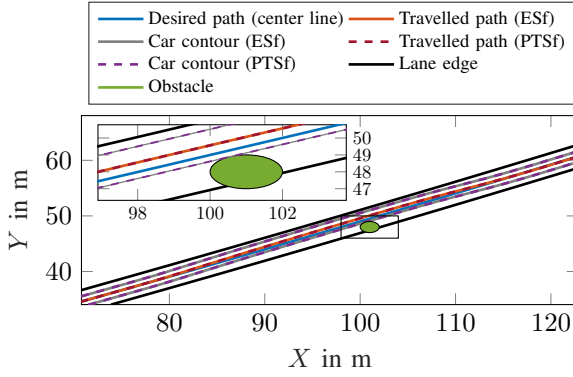


Fig. 2: The OA designs override the MPC control to enforce safety. The ESf filter is tuned to approximately match the performance of the PTSf one. Both designs pass the obstacle at the boundary of the safe set.

the road, even though the desired trajectory would lead to unsafe operation. For the ESf OA design, we select $c_{i,i} = 15$ for $i = \{1, 2\}$ satisfying (10), which allows the vehicle to approach the obstacle very closely (and seemingly match the performance of PTSf); this performance is innate to the PTSf OA design and is desirable because it allows less intervention with the MPC controller, which tracks the desired path well (see Section III-C for a discussion on gain tuning).

We now investigate the control effort required for this OA task. It is clear from Figure 3 that the nominal MPC control input, which seeks to track the centerline, is overwritten by the safety filters to avoid the obstacle. The filters mainly differ early on when safety constraints become active. We observe a large control input generated by the ESf OA design which is undesirable (see [23] for a further discussion). We can alleviate this by lowering the gains $c_{i,i}$ at the cost of increased conservatism, which can become problematic when the lane width is limited, potentially violating the control sharing property. The PTSf OA controller has a significantly smaller peak but allows the vehicle to approach the barrier equally to the ESf OA design. After passing the obstacle, control authority is gradually ceded to the MPC using a smooth step function similar to (5); see [23] for details.

Throughout the maneuver, the control sharing property among the LK and OA controllers was verified. The control inputs are within the input constraint set for all time, but are not designed to do so.

B. PTSf and PT-ICCBF during late obstacle detection

Now suppose that the obstacle is detected when only 15m ahead of the vehicle. We saturate the inputs of the MPC with ESf for LK and PTSf for OA control designs to $|u| \leq u_{\max}$ and compare the results to MPC with the input-constrained equivalent designs following the methodology in Section III-E. Figure 4 illustrates the non-constrained designs steering the vehicle away from the obstacle, but due to the input saturation, violate safety since the vehicle contour intersects with the obstacle. Furthermore, once the obstacle is passed, this design induces oscillations which culminate

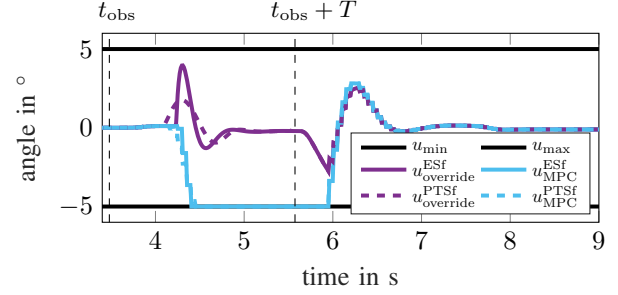


Fig. 3: For similar closed-loop vehicle trajectories, the PTSf filter overrides the MPC control less aggressively than the ESf filter. The discrete-time MPC sends the minimum steering command as the vehicle deviates from the desired trajectory.

in the vehicle driving off the road. In comparison, the ICCBF LK with PT-ICCBF OA design successfully avoids the obstacle while steering the vehicle to the barrier, and additionally, does not cause the vehicle to exit the road after passing the obstacle. Due to the late obstacle detection, the control inputs for both safety filters in Figure 5 are of large amplitude and are saturated at their maximum for much of the time. Despite being saturated, the ICCBF for LK with PT-ICCBF for OA controller ensures safe vehicle operation regardless of being saturated to the maximum allowable, whereas this same input saturation renders the controller absent of the input-constrained design consideration unsafe.

VI. CONCLUSION AND ACKNOWLEDGEMENTS

Our multi-layer MPC and CBF-Safety design exploits the advantages (numerical cost, nonlinear-model-based control fidelity, and ability to perform swift interventions) of both control strategies while allowing the encoding of safety prioritization of OA over LK. This prioritization allows us to establish CBF-QP feasibility, but is conservative, as our simulation studies which do not require any prioritization, show. Additional to ESf filter designs, we explore PTSf and input-constrained safety designs, which bring the advantages of retaining safety while balancing performance, and practicality. Our ongoing research aims to provide some theoretical guarantees for the combinations of ESfs, PTSfs and their input-constrained counterparts for simultaneous LK and OA.

The authors thank Imoleayo Abel and Bob Bitmead for fruitful discussions and valuable comments.

REFERENCES

- [1] J. Rawlings and D. Mayne, *Model Predictive Control: Theory and Design*. Nob Hill Pub., 2009.
- [2] J. Kabzan, L. Hewing, A. Liniger, and M. N. Zeilinger, "Learning-based model predictive control for autonomous racing," *IEEE Robotics and Automation Letters*, vol. 4, no. 4, pp. 3363–3370, 2019.
- [3] R. Zhang, F. Rossi, and M. Pavone, "Model predictive control of autonomous mobility-on-demand systems," in *2016 IEEE International Conference on Robotics and Automation (ICRA)*, pp. 1382–1389, 2016.
- [4] P. Falcone, M. Tufo, F. Borrelli, J. Asgari, and H. E. Tseng, "A linear time varying model predictive control approach to the integrated vehicle dynamics control problem in autonomous systems," in *2007 46th IEEE Conference on Decision and Control*, pp. 2980–2985, 2007.

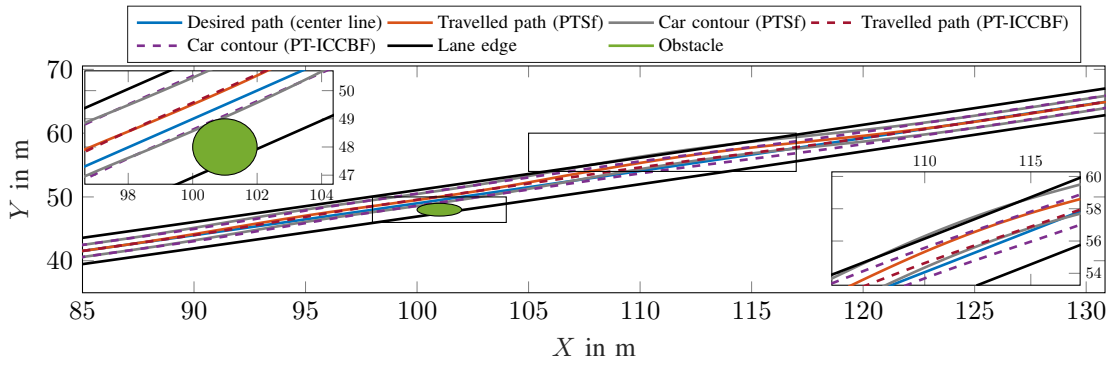


Fig. 4: The vehicle leaves the desired trajectory to avoid the obstacle. The ICPTSf renders the closed loop safe. On the contrary, the zooms reveal that the PTSf violates safety (both of the road barrier and the obstacle) due to saturated control inputs.

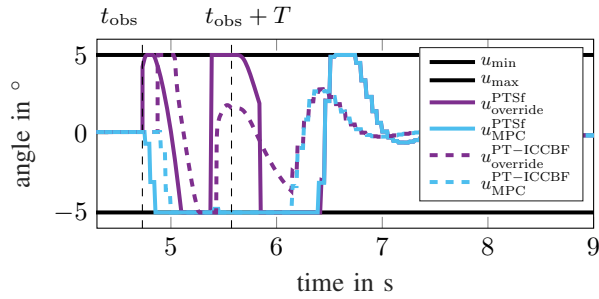


Fig. 5: For a similar trajectory the PT safety filter shows a smoother interjection with less jerk. We also observe the discrete-time nature of the MPC, which sends the minimum steering command as the vehicle is off the desired trajectory.

[5] U. Rosolia, A. Carvalho, and F. Borrelli, "Autonomous racing using learning model predictive control," in *2017 American Control Conference (ACC)*, pp. 5115–5120, 2017.

[6] Q. Nguyen and K. Sreenath, "Exponential control barrier functions for enforcing high relative-degree safety-critical constraints," in *2016 American Control Conference (ACC)*, pp. 322–328, IEEE, 2016.

[7] M. Krstic and M. Bement, "Nonovershooting control of strict-feedback nonlinear systems," *IEEE Transactions on Automatic Control*, vol. 51, no. 12, pp. 1938–1943, 2006.

[8] D. Steeves, M. Krstic, and R. Vazquez, "Prescribed-time h_1 -stabilization of reaction-diffusion equations by means of output feedback," in *2019 18th European Control Conference (ECC)*, pp. 1932–1937, IEEE, 2019.

[9] D. Steeves and M. Krstic, "Prescribed-time stabilization robust to measurement disturbances," in *2022 American Control Conference (ACC)*, p. to appear, IEEE, 2022.

[10] I. Abel, D. Steeves, and M. Krstic, "Prescribed-time safety design for a chain of integrators," *arXiv preprint arXiv:2201.09447*, 2022.

[11] X. Xu, J. W. Grizzle, P. Tabuada, and A. D. Ames, "Correctness guarantees for the composition of lane keeping and adaptive cruise control," *IEEE Transactions on Automation Science and Engineering*, vol. 15, no. 3, pp. 1216–1229, 2018.

[12] R. Rajamani, *Vehicle Dynamics and Control*. Mechanical Engineering Series, Springer US, 2011.

[13] M. Cavorsi, M. Khajenejad, R. Niu, Q. Shen, and S. Z. Yong, "Tractable compositions of discrete-time control barrier functions with application to lane keeping and obstacle avoidance," *arXiv preprint: 2004.01858*, 2020.

[14] Z. Wu, F. Albalawi, Z. Zhang, J. Zhang, H. Durand, and P. D. Christofides, "Control lyapunov-barrier function-based model predictive control of nonlinear systems," in *2018 Annual American Control Conference (ACC)*, pp. 5920–5926, 2018.

[15] K. Garg, R. K. Cosner, U. Rosolia, A. D. Ames, and D. Panagou, "Multi-rate control design under input constraints via fixed-time barrier functions," *IEEE Control Systems Letters*, vol. 6, pp. 608–613, 2022.

[16] T. D. Son and Q. Nguyen, "Safety-critical control for non-affine nonlinear systems with application on autonomous vehicle," in *2019 IEEE 58th Conference on Decision and Control (CDC)*, pp. 7623–7628, 2019.

[17] J. Zeng, B. Zhang, and K. Sreenath, "Safety-critical model predictive control with discrete-time control barrier function," in *2021 American Control Conference (ACC)*, pp. 3882–3889, 2021.

[18] J. Zeng, Z. Li, and K. Sreenath, "Enhancing feasibility and safety of nonlinear model predictive control with discrete-time control barrier functions," *arXiv preprint:2105.10596*, 2021.

[19] X. Xu, "Constrained control of input-output linearizable systems using control sharing barrier functions," *Automatica*, vol. 87, pp. 195–201, 2018.

[20] A. D. Ames, X. Xu, J. W. Grizzle, and P. Tabuada, "Control barrier function based quadratic programs for safety critical systems," *IEEE Transactions on Automatic Control*, vol. 62, no. 8, pp. 3861–3876, 2016.

[21] S.-C. Hsu, X. Xu, and A. D. Ames, "Control barrier function based quadratic programs with application to bipedal robotic walking," in *2015 American Control Conference (ACC)*, pp. 4542–4548, IEEE, 2015.

[22] G. Wu and K. Sreenath, "Safety-critical and constrained geometric control synthesis using control lyapunov and control barrier functions for systems evolving on manifolds," in *2015 American Control Conference (ACC)*, pp. 2038–2044, IEEE, 2015.

[23] I. Abel, D. Steeves, and M. Krstic, "Prescribed-time safety design for a chain of integrators," in *American Control Conference (ACC)*, 2022.

[24] D. Agrawal and D. Panagou, "Safe control synthesis via input constrained control barrier functions," *arXiv preprint arXiv:2104.01704*, 2021.

[25] F. Borrelli, A. Bemporad, and M. Morari, *Predictive Control for Linear and Hybrid Systems*. Cambridge University Press, 2017.

[26] E. Gilbert and K. Tan, "Linear systems with state and control constraints: the theory and application of maximal output admissible sets," *IEEE Transactions on Automatic Control*, vol. 36, no. 9, pp. 1008–1020, 1991.

[27] B. Kouvaritakis and M. Cannon, *Model Predictive Control: Classical, Robust and Stochastic*. Advanced Textbooks in Control and Signal Processing, Springer International Publishing, 2015.

[28] D. Mayne, J. Rawlings, C. Rao, and P. Scokaert, "Constrained model predictive control: Stability and optimality," *Automatica*, vol. 36, no. 6, pp. 789–814, 2000.

[29] D. Limon, T. Alamo, F. Salas, and E. Camacho, "On the stability of constrained mpc without terminal constraint," *IEEE Transactions on Automatic Control*, vol. 51, no. 5, pp. 832–836, 2006.

[30] P. Camille Thomason, "Roadway design manual," http://onlinemanuals.txdot.gov/txdotmanuals/rdw/manual_noti, 2020. [Accessed May 2022].